Cellular/Molecular

Organization of Functional Synaptic Connections between Medullary Reticulospinal Neurons and Lumbar Descending Commissural Interneurons in the Neonatal Mouse

Karolina Szokol, Joel C. Glover, and Marie-Claude Perreault
University of Oslo, Institute of Basic Medical Sciences (Domus Medica), Department of Physiology, N-0317 Oslo, Norway

The medullary reticular formation (MRF) of the neonatal mouse is organized so that the medial and lateral MRF activate hindlimb and trunk motoneurons (MNs) with differential predominance. The goal of the present study was to investigate whether this activation is polysynaptic and mediated by commissural interneurons with descending axons (dCINs) in the lumbar spinal cord. To this end, we tested the polysynapticity of inputs from the MRF to MNs and tested for the presence of selective inputs from medial and lateral MRF to 574 individual dCINs in the L2 segment of the neonatal mouse.

Reticulospinal-mediated postsynaptic Ca^{2+} responses in MNs were reduced in the presence of mephenesin and after a midline lesion, suggesting the involvement of dCINs in mediating the responses. Consistent with this, stimulation of reticulospinal neurons in the medial or lateral MRF activated 51% and 57% of ipsilateral dCINs examined (255 and 352 dCINs, respectively) and 52% and 46% of contralateral dCINs examined (166 and 133 dCINs, respectively). The proportion of dCINs that responded specifically to stimulation of medial or lateral MRF was similar to the proportions of dCINs that responded to both MRF regions or to neither. The three responsive dCIN populations had largely overlapping spatial distributions.

We demonstrate the existence of dCIN subpopulations sufficient to mediate responses in lumbar motoneurons from reticulospinal pathways originating from the medial and lateral MRF. Differential control of trunk and hindlimb muscles by the medullary reticulospinal system may therefore be mediated in part by identifiable dCIN populations.

Introduction

The mammalian reticulospinal system, composed of medullary and pontine reticulospinal neurons, plays a crucial role in initiating locomotion and associated postural control (Grillner et al., 1995; Mori et al., 1995; Drew et al., 2004; Garcia-Rill et al., 2004; Matsuyama et al., 2004a; Sasaki et al., 2004; Deliagina et al., 2006, Jordan et al., 2008). This is thought to be achieved through the extensive branching of reticulospinal axons (Peterson et al., 1975; Matsuyama et al., 1993, 1997; Sasaki, 1997), allowing them to exert widespread direct and indirect actions on spinal motoneurons (MNs) (Grillner and Lund, 1968; Grillner et al., 1968; Shapovalov, 1969; Wilson and Yoshida, 1969; Peterson, 1979; Peterson et al., 1979; Floeter et al., 1993; Sasaki, 1999; Habaguchi et al., 2002; Jankowska et al., 2003; Alstermark and Ogawa, 2004; Alstermark et al., 2004; Riddle et al., 2009). However, the identities of the spinal interneurons (INs) that mediate reticulospinal actions on MNs remain elusive (for surveys of reticulospinal actions on interneurons identified by proprioceptive inputs, see Jankowska, 1992; Jankowska and Edgley, 2010).

Initiation of locomotion by reticulospinal neurons probably relies on the activation of excitatory INs in the lumbar spinal cord (Brownstone and Wilson, 2008; Kiehn et al., 2008; Hägglund et al., 2010). In the mouse spinal cord, two broad populations of excitatory INs have been identified by their intraspinal axonal trajectories and developmental expression of molecular markers: (1) ipsilaterally projecting INs that express the transcription factors HB9 (Hinckley et al., 2005; Wilson et al., 2005), Chx10 (Al-Mosawie et al., 2007; Lundfald et al., 2007), or Sim1 (Zhang et al., 2008; J. C. Glover, unpublished observations); and (2) contralaterally projecting INs (CINs) that express the transcription factors Evx1 (Moran-Rivard et al., 2001; Pierani et al., 2001; Lanuza et al., 2004) or Sim1 (Zhang et al., 2008; Hägglund et al., 2010). It is clearly established in the adult cat that excitatory CINs receive inputs from pontine reticulospinal neurons (Jankowska et al., 2009 and references therein).

Here, we use a recently developed calcium-imaging approach to assess synaptic connections between brainstem and spinal neurons in the neonatal mouse (Szokol et al., 2008; Szokol and Perreault, 2009) to determine whether lumbar CINs receive inputs from medullary reticulospinal neurons. In the neonatal rodent, four classes of CINs can be identified on the basis of contralateral axonal trajectory: intrasegmental (short-range CINs), intersegmental ascending, descending (aCINs, dCINs), and bifurcating [ascending, descending (adCINs)] (Eide et al., 1999; Stokke et al.,

Received Oct. 20, 2010; revised Jan. 28, 2011; accepted Feb. 4, 2011.

This work was supported by grants from the Norwegian Research Council (to M.-C.P. and J.C.G.) and the International Foundation for Research in Paraplegia (to M.-C.P.). K.S. was supported by a fellowship from the Christopher and Dana Reeve Foundation and the Amerisure Charitable Foundation. We thank Kobra Sultani and Marian Berge Andersen for technical assistance and Bruce Piercey for writing the Fileconvert program.

Correspondence should be addressed to Dr. Marie-Claude Perreault, University of Oslo, Institute of Basic Medical Sciences, Department of Physiology, Sognsvannsveien 9, PB 1103 Blindern, N-0317, Oslo, Norway. E-mail: m.c.perreault@basalmed.uio.no.

DOI:10.1523/JNEUROSCI.5486-10.2011

 0270-6474/11/314731-12$15.00/0

2002; Nissen et al., 2005). Since dCINs can be labeled retrogradely with calcium-sensitive probes without compromising the integrity of reticulospinal projections, we have focused on this population. We first show that treatment with mephenesin to diminish the efficacy of polysynaptic pathways and midline lesions to interrupt local commissural projections both reduce reticulospinal-mediated postsynaptic Ca^{2+} responses in MNs. Second, we show that activation of reticulospinal neurons elicits postsynaptic Ca^{2+} responses in individual dCINs in a selective pattern. We then relate the selective organization of reticulospinal connections to MNs to that of dCINs. Preliminary accounts of some of this work have appeared previously (Perreault et al., 2009; Szokol and Perreault, 2009; Szokol et al., 2009).

Materials and Methods

Brainstem–spinal cord preparation. Experiments were performed on isolated brainstem–spinal cord preparations ($n = 47$) from neonatal [postnatal day (P) 0–P5] ICR mice (Harlan). Animals were deeply anesthetized with isoflurane, decerebrated, and eviscerated. The brainstem and the spinal cord were exposed by craniotomy and laminectomy. The brainstem–spinal cord with attached ventral roots was then gently dissected out in an ice-cold (1–5°C), oxygenated (95% O_2 and 5% CO_2), glycerol-based dissection solution containing the following (in mM): glycerol 250, KCl 2, D-glucose 11, $CaCl_2$ 0.15, $MgSO_4$ 2, NaH_2PO_4 1.2, HEPES 5, and $NaHCO_3$ 25.

All efforts were made to minimize the number of animals used and their suffering, in accordance with the European Communities Council directive 86/609/EEC and the National Institutes of Health guidelines for the care and use of animals. The procedures were approved by the National Animal Research Authority in Norway.

Retrograde labeling. To retrogradely label MNs and dCINs in the L2 segment, we applied crystals of calcium green-1-conjugated dextran amine (CGDA; 3000 MW, Invitrogen) to the cut end of their axons. For the MNs, the axons were cut close to the ventral root exit from the spinal cord to minimize labeling time. For the dCINs (and possibly a few adCINs, which were labeled together with dCINs), the axons were cut at the border between the L3 and L4 segments (Fig. 1*A*), restricting the cut to the ventral funiculus (Glover, 1995; Nissen et al., 2005; Szokol and Perreault, 2009). The dissection solution was then replaced by oxygenated artificial CSF containing the following (in mM): NaCl 128, KCl 3, D-glucose 11 $CaCl_2$ 2.5, $MgSO_4$ 1, NaH_2PO_4 1.2, HEPES 5, and $NaHCO_3$ 25. Retrograde labeling continued in the dark at room temperature (23–25°C) for 3 h (MNs) or 5 h (dCINs).

Optical recording of calcium transients. For imaging MNs, the brainstem–spinal cord preparation containing the labeled MNs was transferred to a recording chamber where it was pinned down with the ventral side up. For imaging dCINs, an additional transection at the mid-L2 segment was performed before the transfer of the preparation to the recording chamber. The transection to expose the dCINs was made in an oblique plane from the ventral to the dorsal surface with an angle between 50° and 60° from the horizontal and the transected end was positioned on a Sylgard block so that the obliquely cut surface lay horizontally under the objective (for more details, see Szokol and Perreault, 2009). We recorded fluorescent signals in dCINs from this obliquely cut, face-up configuration (Fig. 1*B*) using a 40× water-immersion objective (LUMPlanFl, 0.8 NA; Olympus) on an epifluorescence microscope (Axioskop or Axioskop FS-2; Carl Zeiss) equipped with a 100 W halogen lamp.

Changes in fluorescence intensity were detected using a CCD camera (Cascade 650; Photometrics) mounted on a video zoom adaptor. Video images were acquired using image-processing software (MetaMorph 5.0; Molecular Devices). To minimize photobleaching and phototoxicity, we typically used low intensity epi-illumination, a frame rate of 4 Hz, and a gain and a binning factor of 3. We also limited the exposure time per recording to 2 min. In some experiments ($n = 8$), we used a higher frame rate (80.2–197 Hz) and higher binning (3–6) to record more accurately the latencies of the responses in dCINs. However, such high frame rate

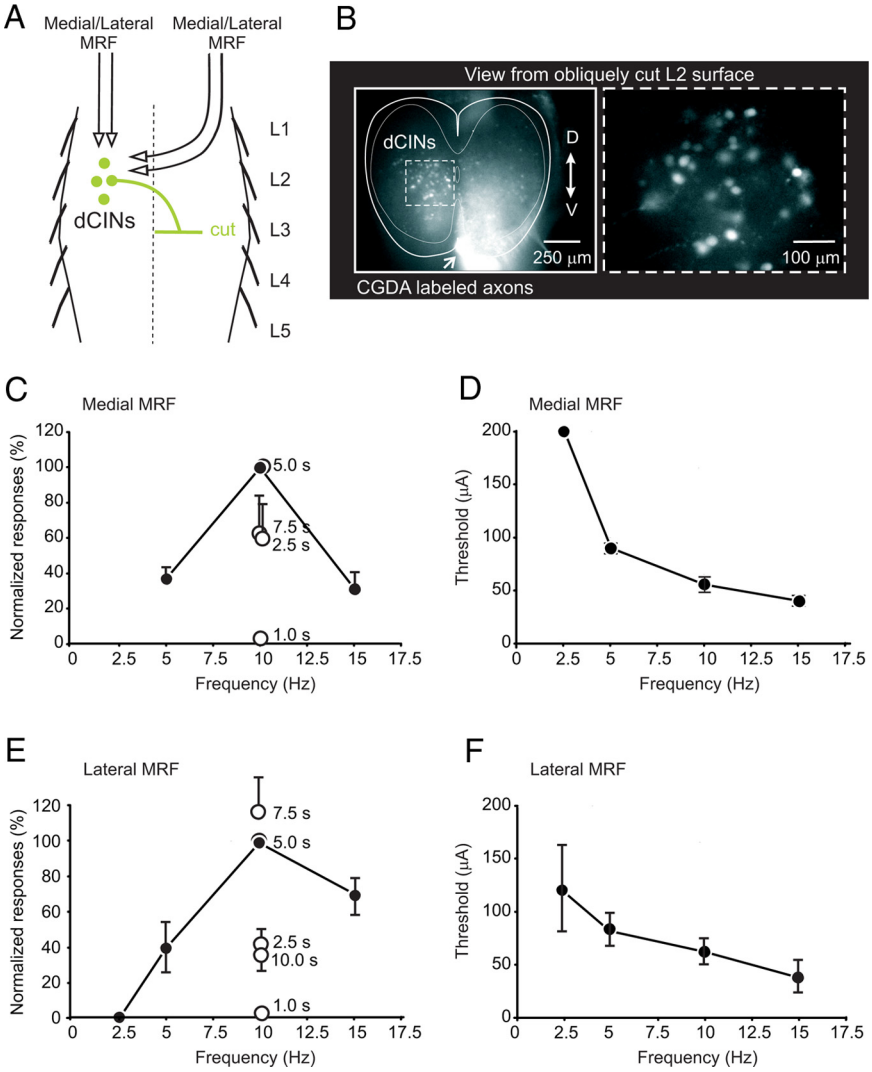

Figure 1. Labeling and visualization of L2 dCINs in the obliquely cut, face-up brainstem–spinal cord preparation and effective stimulation parameters. ***A***, Putative connections examined between medial and lateral MRF and dCINs. The connections may represent monosynaptic and/or polysynaptic connections. ***B***, Low-magnification microphotograph showing CGDA-labeled dCINs (and axons in the ventral funiculus) from the cut surface of the L2 spinal segment in the obliquely cut, face-up brainstem–spinal cord preparation. The boxed area (left) is displayed at a higher magnification (right) and shows that individual dCINs can be clearly visualized. ***C–F***, Effective stimulation parameters for evoking Ca^{2+} responses in ipsilateral dCINs with stimulation of the medial MRF (***C***, ***D***, $n = 7–12$ dCINs in each of in four preparations) and with stimulation of the lateral MRF (***E***, ***F***, $n = 10–29$ dCINs in each of four preparations). ***C***, ***E***, Response magnitude–frequency curves when stimulating at 2 T and 5 s train duration (filled circles) and the response magnitudes at different train durations (individual, open circles) with otherwise the same stimulation parameters. ***D***, ***F***, Response magnitudes evoked by stimulation with a 5 s train at threshold current (T) as a function of frequency. D, Dorsal; V, ventral.

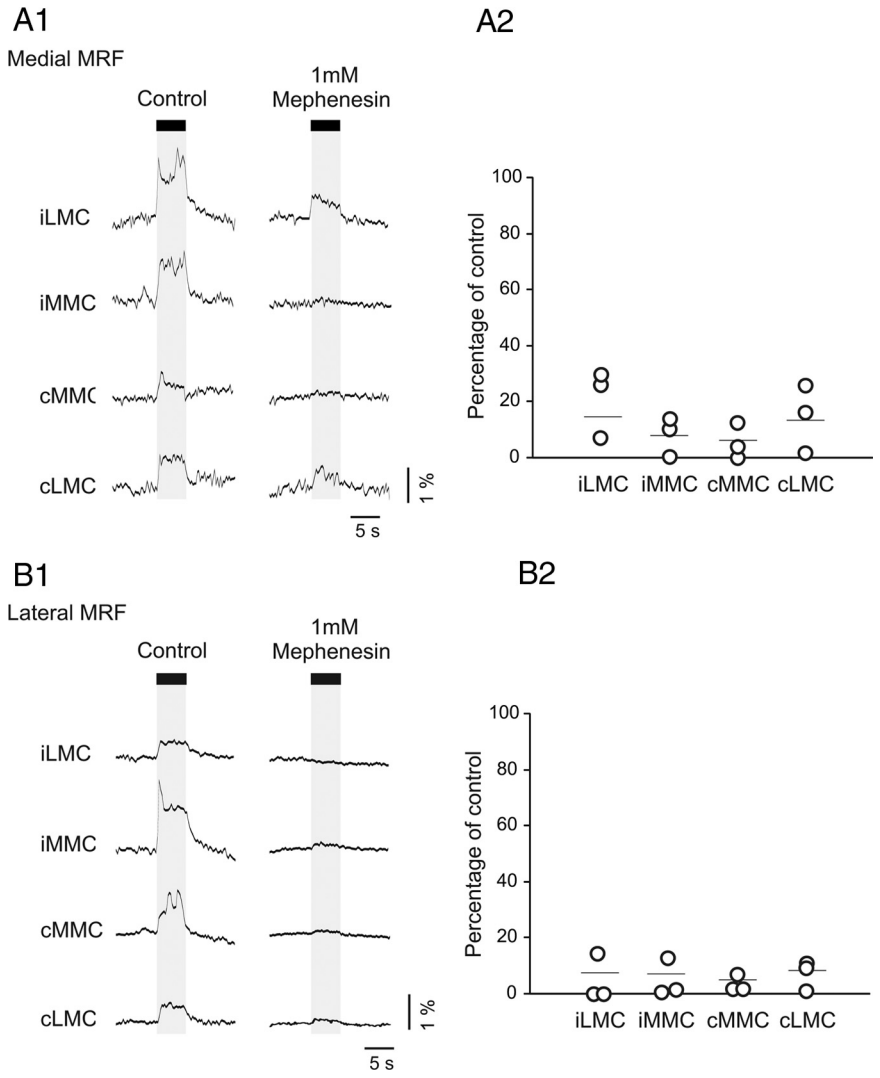

Figure 2. Mephenesin strongly reduces the magnitude of the MRF-evoked responses in L2 MNs. ***A1***, ***B1***, Responses evoked during electrical stimulation of the medial MRF and lateral MRF with a 5 s train at 10 Hz (2 T) in the MNs of the iLMC, iMMC, cMMC, and cLMC before (left) and after (right) application of mephenesin to a split-bath compartment containing the cervico-thoracolumbar region of the spinal cord. Because individual labeled MNs are easily visualized through the ventral white matter, all optical recordings from MNs were performed in intact brainstem–spinal cord preparations (Szokol et al., 2008; Szokol and Perreault, 2009). ***A2***, ***B2***, Corresponding graphs showing the magnitudes of the responses during mephenesin application, normalized to the control response. Each point shows the average response in a single preparation and the horizontal lines indicate the grand mean.

recordings, because they require higher intensity illumination, led to substantial photobleaching of the CGDA and therefore could not be done routinely or for long periods.

Electrical stimulation. Electrical stimulation of the medullary reticular formation (MRF) was delivered with a monopolar tungsten microelectrode [shaft diameter, 0.356 mm; tip diameter, 1–2 μm; impedance, 0.1 MΩ at 1 kHz; World Precision Instruments (WPI)] using a DS8000 stimulator (WPI) coupled to an isolation unit (ISOFlex; AMPI). In approximately half of the preparations, more than one MRF regions were stimulated. At the beginning of each experiment, the medial and/or lateral MRF region was tracked with the electrode until a response was observed in L2 MNs/dCINs. During this initial search for effective stimulation sites, we used stimulation strengths of 200 μA. At each effective site, we delivered two stimulation trains (5 s duration, 200 μs pulse at 10 Hz, 15–200 μA). The two trains were delivered at 10 and 70 s or 40 and 100 s after the onset of the 120 s optical recording session. Stimulation strength was expressed in multiples of threshold (T) for evoking a detectable increase in fluorescence (see Measurement of calcium responses, below). At the end of the experiment, an electrolytic lesion (60 μA for 3 s at P0–P3 or 5 s at P4–P5, cathodal followed by anodal DC) was made at the deepest stimulation site along the last electrode track. We also marked the electrode tracks by coating the stimulating electrode before each experiment with a saturated DiI solution (for more details, see Szokol and Perreault, 2009).

In a series of control experiments, we tested whether the most effective stimulation parameters for evoking reticulospinal responses in lumbar MNs (Szokol et al., 2008; Szokol and Perreault, 2009) also effectively evoked responses in dCINs. This was done by stimulating the medial and lateral regions of the ipsilateral MRF with various train durations and frequencies (Fig. 1*C–F*). We found that, as with MNs, stimulation with 5 s trains was more effective in evoking detectable Ca^{2+} transients in dCINs than stimulation with trains of shorter duration, whereas prolonging the train duration further decreased the magnitude of the responses (Fig. 1*C*,*E*, individual points). In both MRF regions, the response magnitudes using 5 s stimulus trains peaked at 10 Hz (Fig. 1*C*,*E*, magnitude-frequency curves) and the stimulus intensity threshold to elicit detectable responses (T) decreased with increasing frequency (Fig. 1*D*,*F*). Thus, the stimulation parameters that we previously found to be most effective in eliciting response in MNs also efficiently elicited responses in dCINs.

Histological localization of stimulation sites. Histological processing of the brainstem was performed after 12–20 h fixation in 4% paraformaldehyde, cryoprotection in 20% sucrose, and cryostat sectioning (serial sections of 50 μm in the transverse plane). Sections were stained with Harris hematoxylin (Histolab) and subsequently examined for electrolytic lesions and DiI traces. The sections containing electrolytic lesions and DiI traces were photographed with a ProgRes C14 camera (Jenoptik) mounted on an Olympus AX70 microscope and used to measure the position of the effective stimulation sites. Effective stimulation sites were plotted on standard anatomical sections of the P0 mouse brainstem adapted and modified from Paxinos et al. (2007). Age-related differences in the size of the brainstem were taken into account when plotting the sites onto the standardized sections.

Measurement of calcium responses. The timing markers for the brainstem stimulation and the gating pulse from the CCD camera were recorded at 500 Hz (Digidata1320A; Molecular Devices). To synchronize the electrical and the optical recordings, a digital pulse from the Digidata unit was sent to the CCD camera. In each experiment, our analysis was restricted to the focal plane that contained the largest number of clearly visible MNs or dCINs. In principle, however, it would have been possible to analyze responses from more MNs/dCINs visible in other focal planes. After each recording, regions of interest (ROIs) were placed manually over the somata of easily distinguishable labeled MNs or dCINs (six MNs in each motor column and 6–30 dCINs). The selection of MNs/dCINs was always done on the first frame of the recording and therefore was blind to the effect of the stimulation. The fluorescence intensity averaged over all the pixels in each ROI was measured in each image frame. To account for differences in labeling intensity among different MNs/dCINs, the Ca^{2+} transients in each ROI were expressed as changes in fluorescence intensity divided by the prestimulus baseline intensity [$\Delta F/F = (F - F_{baseline})/F_{baseline}$]. We have previously evaluated the extent to which light scattering from an

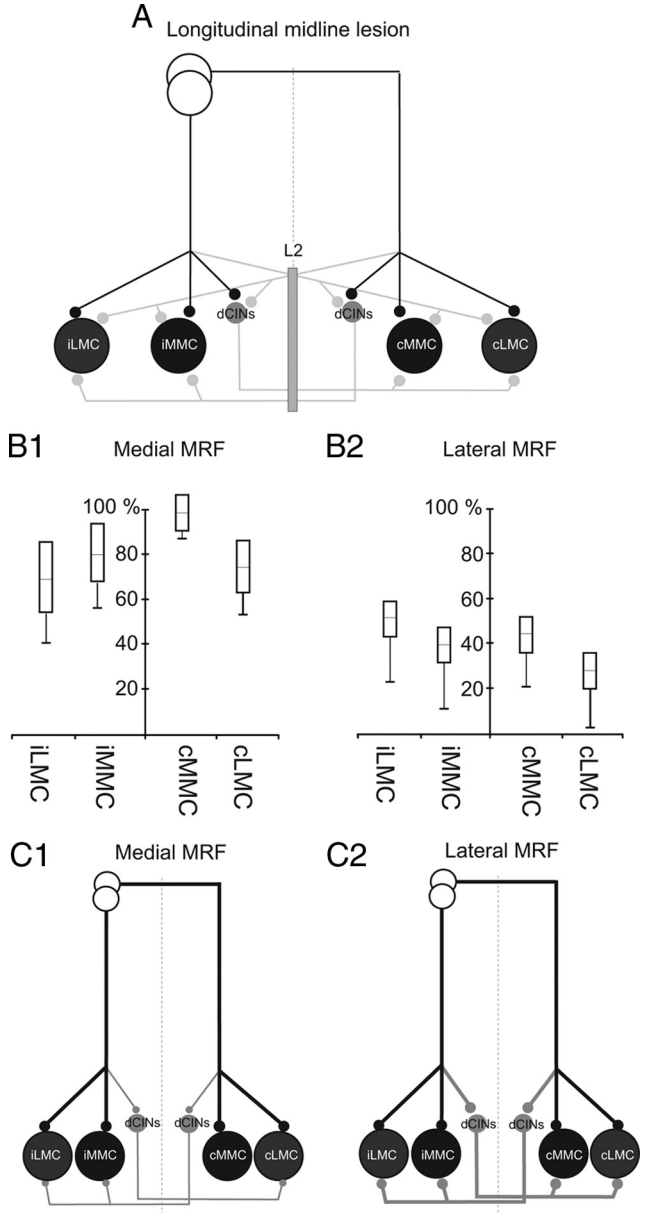

Figure 3. L2 midline lesions decrease the magnitudes of the MRF-evoked responses in L2 MNs. ***A***, Putative excitatory connections between bilaterally projecting medullary reticulospinal neurons and L2 MNs of the iLMC, iMMC, cMMC, and cLMC. Putative connections rendered ineffective by the L2 midline lesion (gray rectangle) are shown as light gray elements. All connections may represent monosynaptic and/or polysynaptic connections. ***B1***, ***B2***, Effect of a longitudinal section of the midline at L2 on the responses evoked in L2 MNs by stimulation of the medial (***B1***, $n = 3$) and lateral (***B2***, $n = 3$) MRF. For each MN group, the response that remained after L2 midline lesion, expressed as a percentage of the control response, is shown in the form of box-and-whisker diagrams: mean (horizontal line), SEM (box), and SD (vertical line). ***C1***, ***C2***, Connectivity diagrams deduced from the lesion experiments. For each MN group, the principal connections are shown as thicker lines. In these schemes, interposed synaptic connections are not included and all crossing connections within the spinal cord are assumed to be mediated by dCINs. Crossing collaterals of reticulospinal or propriospinal axons might also be involved but this possibility remains to be tested.

activated MN in the *x–y* plane could give false-positive response in adjacent MNs when recording at 4 Hz (Szokol et al., 2009). We performed a similar analysis for dCINs in four experiments and found that responses recorded from single dCINs spatially isolated from the main population of labeled dCINs fell off by 60% over a distance of one dCIN soma diameter (mean dCIN soma diameter, 13 ± 1 μm; $n = 50$) and by 80% over a distance of two soma diameters.

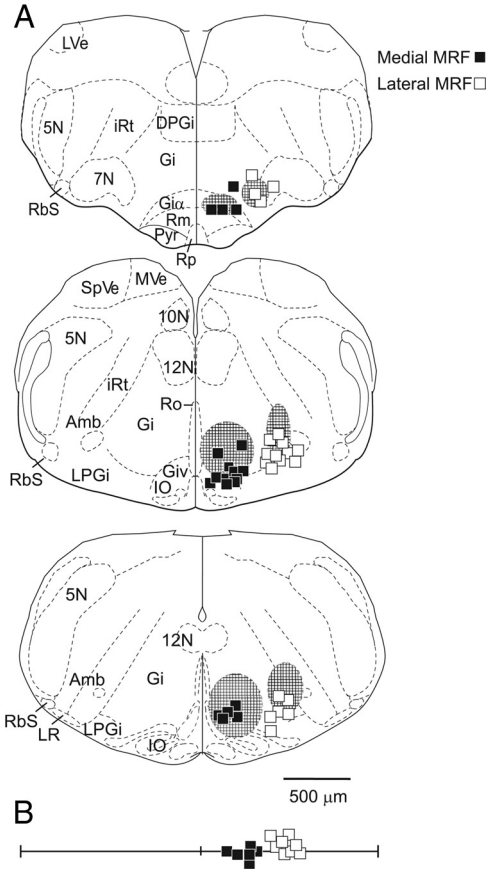

Figure 4. Locations of effective stimulation sites in the MRF. ***A***, Stimulation sites recovered from transverse brainstem sections and plotted directly on standardized sections from a P0 mouse (adapted and modified from Paxinos et al., 2007) at three different anteroposterior levels. In all of these experiments, the locations of the stimulation sites were confirmed histologically from electrolytic lesions and DiI tracks left by the electrode trajectory (see Materials and Methods). The effective sites in the medial and lateral MRF regions are plotted as filled and unfilled squares, respectively. Cross-hatched areas indicate the regions that were previously found to be effective in evoking responses in the MMC and LMC (Szokol et al., 2008). 5N, Spinal trigeminal nucleus; 7N, facial nucleus; 10N, dorsal motor nucleus of the vagus; 12N, hypoglossal nucleus; Amb, ambiguus nucleus; DPGi, dorsal paragigantocellularis nucleus; Gi, gigantocellularis reticular nucleus; Giα, pars α; Giv, pars ventralis; IO, inferior olive nucleus; LPGi, lateral paragigantocellularis nucleus; LVe, lateral vestibular nucleus; LR, lateral reticular nucleus; iRt, intermediate reticular nucleus; MVe, medial vestibular nucleus; Pyr, pyramidal tract; RbS, rubrospinal tract; Rm, raphe nucleus magnus; Ro, raphe nucleus obscurus; Rp, raphe nucleus pallidus; SpVe, spinal vestibular nucleus. ***B***, Additional effective sites for which electrolytic lesions were ambiguous or missing but mediolateral positions could be obtained from photographs of the electrodes positions during experiments. Scale bar: ***A***, ***B***, 500 μm.

Data in the video files were converted to text files using a custom made program (FileConvert), imported into Clampfit 9.2 (Molecular Devices) and expressed as waveforms. The magnitudes of the responses were measured by calculating the areas under the waveforms that exceeded the mean value of the prestimulus baseline by 2 SD. Responses that were contaminated by spontaneous activity were not analyzed. Response magnitudes were then exported to Microsoft Office Excel 2007 for further analysis and graphical display. Alignment of optical waveforms and stimulus markers in the illustrations was done manually using Corel Draw X4. Unless stated otherwise, data are given as mean ± SEM.

Results

Effect of mephenesin and midline lesions on MRF-evoked responses in L2 MNs

To test the idea that spinal dCINs might participate in the production of the MRF-mediated responses evoked in MNs, we first

examined the effects of mephenesin, a drug that reduces transmission in descending polysynaptic pathways (Floeter and Lev-Tov, 1993; Vinay et al., 1995; Juvin and Morin, 2005). The stimulating electrode was targeted to the same two regions of the MRF, which we previously denoted "medial MRF" and "lateral MRF" and which exert differential effects on MNs of the medial and lateral motor columns (MMC and LMC, respectively) in L2 and L5 segments (Szokol et al., 2008; Szokol and Perreault, 2009). Mephenesin was bath-applied to the spinal cord after isolating it from the brainstem with a vaseline barrier made at C1 ($n = 6$).

As shown in Figure 2*A1*, mephenesin (1 mM) greatly decreased the responses evoked by the medial MRF in MNs of all four motor columns. On average, the response in the ipsilateral MMC and LMC (iMMC and iLMC) was decreased by 92% and 84%, respectively, and, in the contralateral MMC and LMC (cMMC and cLMC), by 94% and 85%, respectively (Fig. 2*A2*). In many but not all MNs, the response was completely eliminated (6 of 18 MNs in iMMC, 1 of 30 in iLMC, 18 of 28 in cMMC, and 17 of 30 in cLMC).

The effects of mephenesin on the responses evoked by the lateral MRF (Fig. 2*B1*,*B2*) were qualitatively similar with an average decrease in response of 95% and 96% in iMMC and iLMC, respectively, and 97% and 94% in cMMC and cLMC, respectively. The number of MNs in which the response was completely eliminated after application of mephenesin was 10 of 18 in iMMC, 12 of 18 in iLMC, and 8 of 18 in each of cMMC and cLMC.

Together, these findings suggest that activation of L2 MNs by medullary reticulospinal neurons in the neonatal mouse is mediated substantially, in some cases exclusively, through disynaptic and polysynaptic pathways. Floeter and Lev-Tov (1993) made a similar suggestion with regard to activation of lumbar MNs by pontine reticulospinal neurons in the neonatal rat.

We then examined the effect of midline lesions on the responses in L2 MNs evoked by stimulation of the MRF. As depicted in Figure 3*A*, many crossed and uncrossed pathways (including dCIN-mediated pathways) potentially exist between MRF reticulospinal neurons and L2 motor columns. This is because the medial and lateral MRF each project axons down both sides of the spinal cord and both ipsilaterally and contralaterally descending reticulospinal axons may provide inputs to MNs (and dCINs) located on the same side (uncrossed MRF inputs) and/or on the opposite side (crossed MRF inputs) relative to the axon. Because of the potential complexity of the connectivity, the effects of local midline lesions on MN responses evoked by stimulation of the medial and the lateral MRF are described separately.

Local midline lesions decreased the responses evoked by stimulation of the medial MRF by ~20–30% in all L2 motor columns except the contralateral MMC (Fig. 3*B1*). Although reticulospinal inputs to any given motor column may influence each other and give rise to nonlinear and permissive interactions, this result suggests that a combination of uncrossed and crossed inputs from the medial MRF is required to generate responses in all motor columns except the contralateral MMC, for which uncrossed inputs from contralaterally descending axons evidently are sufficient (Fig. 3*C1*).

The effect of midline lesions on responses evoked by stimulation of the lateral MRF was qualitatively similar but the decreases in responses were larger (≥50%) and included decreases in the contralateral MMC (Fig. 3*B2*). This suggests that a combination of crossed and uncrossed inputs from the lateral MRF is required for the production of responses in all motor columns (Fig. 3*C2*).

Table 1. Total number and proportion of responsive ipsilateral and contralateral dCINs following stimulation of the medial and lateral MRF

	Ipsilateral dCINs		Contralateral dCINs	
MRF region stimulated	Medial	Lateral	Medial	Lateral
Responsive	122	182	82	60
Recorded	255	352	166	133
Averaged ratio	51 ± 6% ($n = 15$)	57 ± 6% ($n = 21$)	52 ± 8% ($n = 12$)	46 ± 8% ($n = 9$)

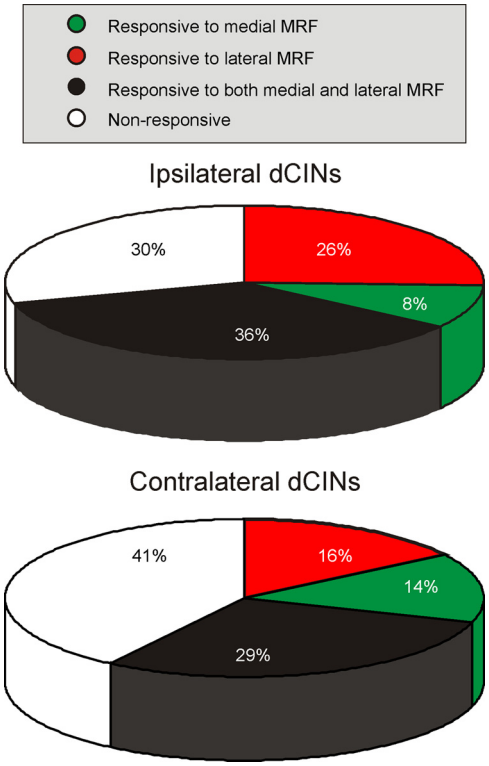

Figure 5. Proportions of ipsilateral and contralateral dCINs with different response patterns to stimulation of medial and lateral MRF. Pie diagrams showing the relative proportions of ipsilateral and contralateral dCINs that responded to medial MRF (green), lateral MRF (red), or both (black) and dCINs that were nonresponsive (white). Data are only from experiments where the effects of medial and lateral MRF stimulation were compared directly on the same group of dCINs. Note that these proportions cannot be equated with the relative importance of the different categories in mediating differential responses in MNs because the connections from dCINs to MNs have not been characterized (neither with respect to strength nor to degree of convergence).

Together, the above findings indicate a clear contribution from disynaptic and/or polysynaptic pathways to MRF-evoked responses in L2 MNs and therefore that at least some of the responses may be mediated by dCINs. Uncrossed and crossed MRF inputs to dCINs could be transmitted by respectively ipsilateral or commissural reticulospinal axon collaterals (Matsuyama et al., 2004b), potentially giving rise to single-crossed and double-crossed dCIN-mediated reticulospinal pathways to lumbar MNs.

Distribution of stimulation sites in the MRF that activate dCINs

As shown in Figure 4, a total of 55 stimulation sites in either the medial or lateral MRF were found to evoke responses in L2 dCINs. The locations of 41 of these sites were confirmed histologically and, as shown, all were located within or in the

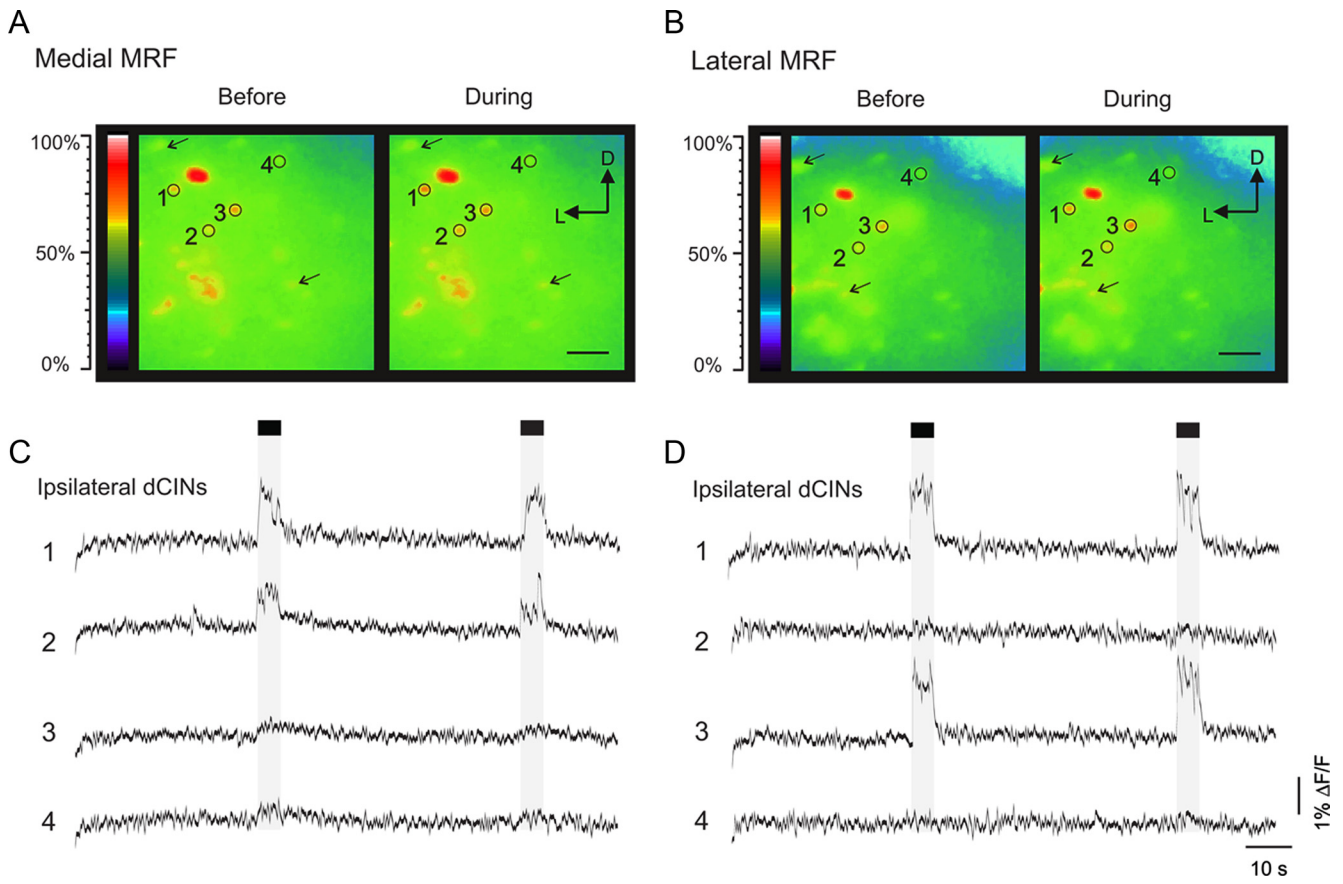

Figure 6. Activation of ipsilateral L2 dCINs following stimulation of the medial and lateral MRF. ***A***, ***B***, Single pseudocolor-coded video frames (pixel intensities filtered with a 3 × 3 median filter and assigned to a rainbow-type color index) showing Ca^{2+} fluorescence in ipsilateral dCINs before and during the first of two trains of stimuli (1.5 T, 5 s) delivered to the medial (***A***) and lateral (***B***) MRF in a P5 mouse. The frames in ***A*** and ***B*** were obtained sequentially but show mostly the same group of dCINs. The changes in fluorescence intensity in individual dCINs are easily detected by the camera but may appear small under simple visual inspection. Therefore, to facilitate their detection, we have added open circles to indicate the location of the four dCINs whose activity is also shown as waveforms in ***C*** and ***D*** and arrows to indicate the location of additional dCINs that responded to the stimulation. D, Dorsal; L, lateral. ***C***, ***D***, Single waveforms showing the changes in Ca^{2+} fluorescence throughout the entire 120 s recording session in the dCINs numbered 1–4 in ***A*** and ***B***. The apparent increase in Ca^{2+} fluorescence in dCIN 3 during stimulation of the medial MRF fell below our detection limit (see Materials and Methods) and therefore dCIN 3 was defined as nonresponsive to medial MRF stimulation. Scale bar, 50 μm.

immediate vicinity of the regions we previously defined as medial MRF and lateral MRF. Although it was not always possible to investigate more than one MRF region during the course of an experiment, in approximately half of the preparations, we stimulated at least two of the four MRF regions (medial and lateral MRF, both ipsilateral relative to the recorded dCINs, $n = 18$; and medial MRF from each side of the midline, $n = 1$). Synaptically mediated Ca^{2+} transients were recorded and analyzed from a total of 574 L2 dCINs.

Reticulospinal inputs to ipsilateral dCINs

The effects of stimulating the medial MRF ($n = 15$ preparations) or lateral MRF ($n = 21$ preparations) were investigated in a total of 255 and 352 ipsilateral dCINs, respectively (partially overlapping samples). Approximately half of the ipsilateral dCINs recorded and analyzed during stimulation of the medial MRF (51 ± 6%) or lateral MRF (57 ± 6%) responded to the stimulation (Table 1). The remaining dCINs did not respond to stimulation of either MRF region. We cannot exclude the possibility that some of these nonresponsive dCINs might have fallen into the responsive dCINs category had our detection threshold been lower or had other sites in the brainstem been stimulated. However, it is unlikely that the lack of response to MRF stimulation was due to a general inability to respond because in three experiments, stimulating the ipsilateral L2 dorsal root (3 or 6 T, 1 or 2 pulses at 10 Hz) evoked Ca^{2+} responses in nearly all of the dCINs (21 of 24) that were nonresponsive to MRF stimulation (data not shown).

In eight of the preparations, we were able to compare directly the effects of stimulation of medial and lateral MRF on the same population of ipsilateral dCINs (142 dCINs) and therefore determine the extent to which the proportions of responsive dCINs overlapped. Overall, we found that 8% (12 of 142) of ipsilateral dCINs were activated by the medial MRF only, 26% (31 of 142) by the lateral MRF only, 36% (51 of 142) by the medial and the lateral MRF, and 30% (42 of 142) did not respond to stimulation of either region (Fig. 5). In each experiment, at least three of these four possible populations of dCINs were observed. Examples of each population of ipsilateral dCIN from a single experiment are shown in Figure 6. Among the 20 neurons analyzed, three were activated by both the medial and the lateral MRF (Fig. 6*C*,*D*, neuron 1), three by the medial MRF only (Fig. 6*C*, dCIN 2) and one by the lateral MRF only (Fig. 6*D*, dCIN 3).

To summarize, we found three populations of ipsilateral dCINs in the L2 segment that could be distinguished by their synaptic inputs from the MRF (i.e., from the medial MRF, the lateral MRF, or from both regions). This finding supports the idea that, as an integral component of a crossed reticulospinal pathway to MNs, dCINs could mediate responses in contralateral

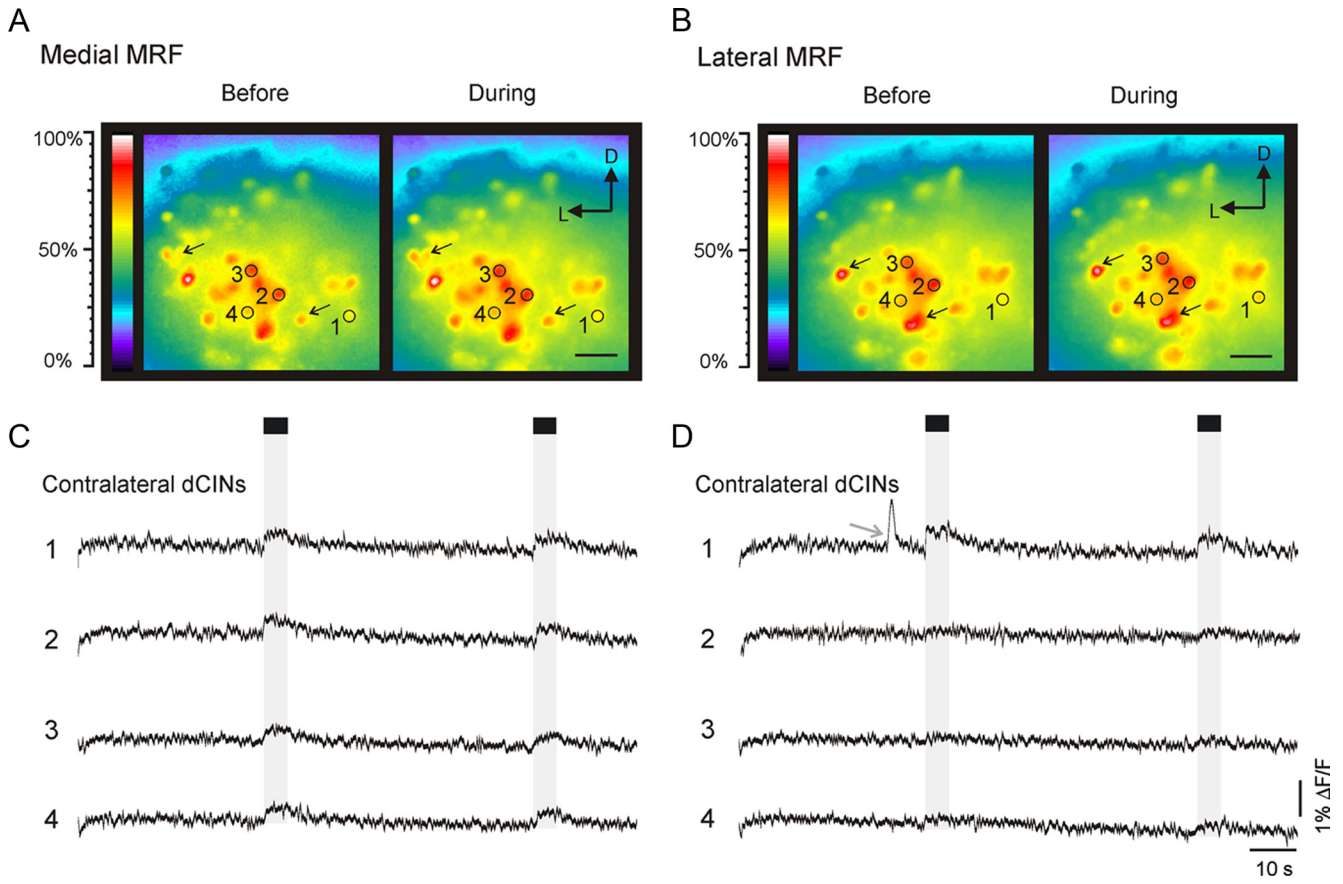

Figure 7. Activation of contralateral L2 dCINs following stimulation of the medial and lateral MRF. ***A***, ***B***, Single pseudocolor-coded video frames showing Ca^{2+} fluorescence in contralateral dCINs before and during stimulation (1.5 T, 5 s) of the medial (***A***) and lateral (***B***) MRF in a P1 mouse. The frames in ***A*** and ***B*** were obtained sequentially but show mostly the same group of dCINs. D, Dorsal; L, lateral. ***C***, ***D***, Single waveforms showing the changes in Ca^{2+} fluorescence in the dCINs numbered 1–4 in ***A*** and ***B***. Scale bar, 50 μm. ***D***, Arrow, Occurrence of a spontaneous Ca^{2+} transient. For other details, see Figure 6.

MNs during stimulation of the MRF (Szokol et al., 2008). The small proportion of ipsilateral dCINs receiving inputs solely from the medial MRF may explain why midline lesion at L2 had little or no effect on the responses evoked in the MNs of the contralateral MMC (see above).

Reticulospinal inputs to contralateral dCINs

The effects of stimulating the medial ($n = 12$ preparations) or lateral ($n = 8$ preparations) MRF was investigated in a total of 166 and 133 contralateral dCINs, respectively (partially overlapping samples). As for the ipsilateral dCINs, approximately half of the contralateral dCINs recorded and analyzed during stimulation of the medial MRF (52 ± 8%) or lateral MRF (46 ± 8%) responded to the stimulation (Table 1). The remaining dCINs did not respond to stimulation of either MRF region.

In eight of the preparations, we were able to compare directly the effects of medial and lateral MRF stimulation on the same population of contralateral dCINs ($n = 133$). Overall, we found that 14% (19 of 133) of the recorded contralateral dCINs were activated by the medial MRF only, 16% (21 of 133) by the lateral MRF only, 29% (39 of 133) by the medial and the lateral MRF, and 41% (54 of 133) did not respond to either of the stimulated MRF regions (Fig. 5). In any given experiment, only three of these four possible populations of dCINs were observed. In the experiment illustrated in Figure 7, of the 23 contralateral dCINs analyzed, three were activated by both the medial and the lateral MRF (Fig. 7*C*,*D*, dCIN 1), nine by the medial MRF only (Fig. 7*C*, dCIN: 2–4), and none by the lateral MRF only.

The results indicate the existence of three populations of contralateral dCINs in the L2 segment with synaptic inputs from either the medial MRF, the lateral MRF, or both. This finding is compatible with the idea that, as part of a double-crossed reticulospinal pathway, dCINs may contribute to the responses evoked in ipsilateral MNs by stimulation of the MRF (Szokol et al., 2008).

Selectivity of connections and minimum latency of responses

To further investigate the selectivity of the connections between medullary reticulospinal neurons and dCINs, we analyzed the responses of subsets of dCINs ($n = 24$) to sequential increases in the number of stimulation pulses from 1 to 2, 3, 5, 25, and 50. This would be expected to recruit more and more dCINs and possibly different sets of dCINs if connections were polysynaptic with variable strengths. Sequential increase from one to five pulses increased the number of dCINs recruited, but no additional recruitment was observed when the pulse number increased to 25 and 50. In the experiment shown in Figure 8, Ca^{2+} responses were examined in seven ipsilateral dCINs during stimulation of the lateral MRF with one pulse (Fig. 8*A*), two pulses (Fig. 8*B*), or 50 pulses (Fig. 8*C*). With one pulse, only one of seven dCINs was activated (Fig. 8*A*, neuron 2) and with two pulses, two additional dCINs were recruited (Fig. 8*B*, neurons 4 and 5). Stimulation with 50 pulses produced larger Ca^{2+} re-

sponse in the dCINs recruited at low stimulus pulse number but did not recruit any additional dCINs. Thus, gradation of MRF stimulation does not lead to substantial recruitment of more dCINs or a shift from one set of recruited dCINs to another, supporting the conclusion that the connections between the two stimulated MRF regions and dCINs are selective.

To investigate the possibility of monosynaptic connections between medullary reticulospinal neurons and dCINs, the latencies of the responses evoked in dCINs were measured after recording the Ca^{2+} transients at high frame rates (130–197 Hz) sufficient to provide a temporal resolution of 5–8 ms ($n = 8$ preparations, total of 80 dCINs). This allowed us to determine approximately the onset of the reticulospinal-evoked Ca^{2+} responses in dCINs because the earliest latencies, as calculated from the start of the train stimulation, were substantially >8 ms regardless of the MRF region stimulated. The ranges of onset latencies are shown in Figure 9 as two separate cumulative plots for the ipsilateral and contralateral dCINs. As shown in Figure 9*A*, 60% of the ipsilateral dCINs activated by the medial MRF responded within the latency range of 38–96 ms and 60% of those activated by the lateral MRF responded within the range of 32–49 ms. For the contralateral dCINs (Fig. 9*B*), the latencies of the responses were longer; 60% of those activated by the medial MRF responded within the latency range of 51–157 ms and 60% of those activated by the lateral MRF responded within the latency range of 45–94 ms. These findings indicate that the shortest latency responses, in ipsilateral dCINs, can be as early as 32 ms (excluding a temporal imprecision of ± 5–8 ms) and raise the possibility that they are produced by monosynaptic inputs from slowly conducting, incompletely myelinated reticulospinal axons (see Discussion, below).

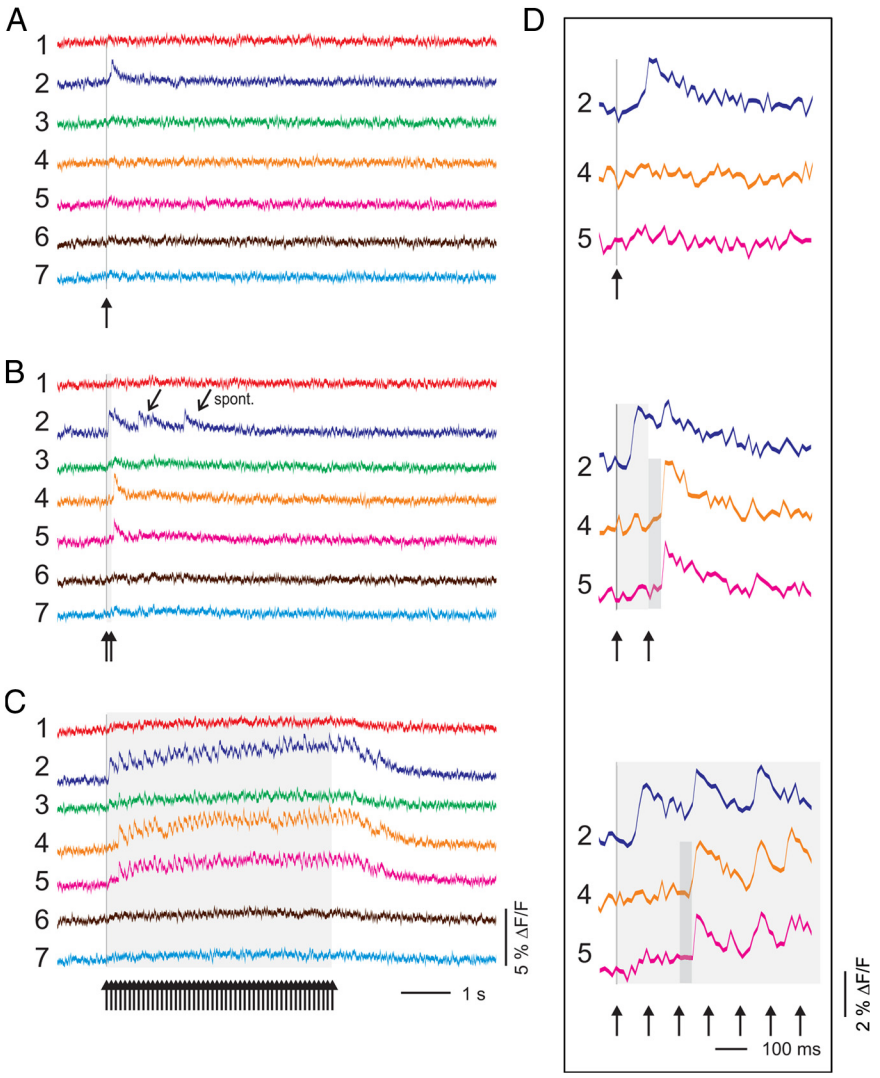

Figure 8. Selective recruitment of dCINs with graded MRF stimulation. ***A–C***, Single waveforms showing Ca^{2+} activity (80 Hz frame rate recording) in seven ipsilateral dCINs during stimulation (2 T, 10 Hz) of the lateral MRF using one pulse (***A***), two pulses (***B***), or 50 pulses (***C***). Stimulation with 50 pulses did not recruit more dCINs than stimulation with two pulses. spont., Spontaneous Ca^{2+} transient. ***D***, Waveform displays of dCINs 2, 4, and 5, taken around the time of the stimulation and shown with a faster time scale. Vertical dark line and light bar indicate the onset and duration of the stimulation and shorter dark bar represents a 40 ms time window from the stimulation pulse immediately preceding the onset of response in dCINs 4 and 5. The response latencies of dCINs 4 and 5, as calculated from the immediately preceding pulse, ranged from 39 to 44 ms, consistent with a possible monosynaptic connection (see Discussion for details).

Together, these results are consistent with the hypothesis that dCINs are involved in mediating disynaptic and polysynaptic excitatory inputs to lumbar MNs from medullary reticulospinal neurons in both the medial and lateral MRF.

Spatial distribution of the recorded dCINs

In a subset of 13 preparations, we could readily recognize the central canal and the midline during optical recording, and used these landmarks to determine the positions of 224 recorded dCINs in the transverse plane. For each dCIN, we measured the radial distance from the middle of the central canal and the angle from the vertical represented by the midline. Figure 10 shows the locations of 28 dCINs that responded to medial MRF stimulation, 43 dCINs that responded to lateral MRF stimulation, 67 dCINs that responded to both MRF regions, and 86 dCINs that did not respond. These dCINs had a spatial distribution similar to that previously reported for dCINs in the mouse embryo [18.5 days old (E18.5)] (Nissen et al., 2005) and for CINs in the neonatal mouse (Restrepo et al., 2009). The majority was located ventral to the midpoint of the central canal, where responsive dCINs predominated over nonresponsive dCINs. There was no obvious segregation of the dCINs that responded to medial MRF, to lateral MRF, or to both.

Discussion

Optical recording in the isolated brainstem–spinal cord of the neonatal mouse has proven useful for characterizing the organization of functional descending connections to spinal MNs (Szokol et al., 2008; Szokol and Perreault, 2009). Here we have exploited this approach to investigate reticulospinal inputs onto a specific class of spinal interneurons, the dCINs (see Introduction, above). We have focused on dCINs located in the L2 segment because this segment is known to have the highest potential for generating rhythmic locomotor activity in the neonatal rat,

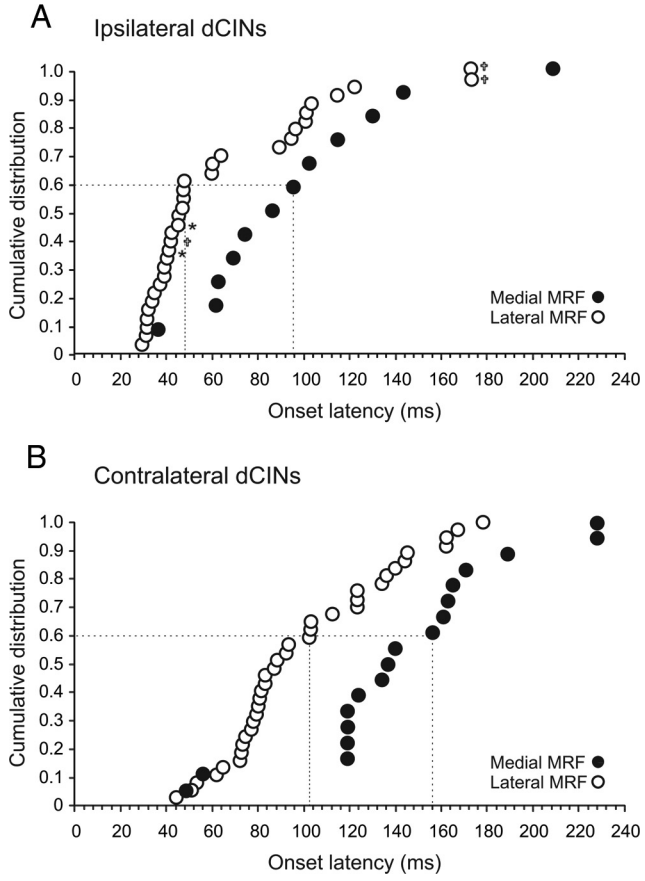

Figure 9. Onset latencies of MRF-evoked responses in L2 dCINs. ***A***, Cumulative distribution of onset latencies of the Ca^{2+} responses evoked in ipsilateral dCINs as calculated from the start of the train stimulation in the medial and lateral MRF. Each point shows the mean response in individual dCINs (responses to two trains). ***B***, Cumulative distribution of onset latencies of the Ca^{2+} responses evoked in contralateral dCINs following train stimulation to the medial and lateral MRF. The Ca^{2+} responses were imaged at a frame rate of 153 Hz except in a few experiments where a frame rate of 130 Hz (crosses) and 197 Hz (stars) was used.

whether induced pharmacologically (Cazalets et al., 1995; Kjaerulff and Kiehn, 1996) or by activation of brainstem descending pathways (Cowley et al., 2009), and because dCINs in this segment are known to mediate inputs onto MNs in more caudal lumbar segments (Butt and Kiehn, 2003).

Our findings support our previous suggestion that dCINs may mediate the pattern of synaptic responses evoked in lumbar MNs by stimulation of the MRF, wherein medial and lateral MRF activate predominantly MNs in the LMC and MMC, respectively (Szokol et al., 2008). First, mephenesin experiments indicate that responses in MNs are mediated mainly polysynaptically via spinal INs and midline lesion experiments implicate CINs as mediators. Second, the stimulation parameters previously found to be most effective for eliciting MRF-mediated responses in lumbar MNs (Szokol et al., 2008) also are most effective for activating dCINs. Third, responsive dCINs can be divided into three populations according to their inputs from the MRF in a pattern that could mediate the full complement of responses evoked in MNs. dCINs responding exclusively to medial or lateral MRF and dCINs responding to both medial and lateral MRF could mediate the predominant responses in MNs of the LMC or MMC. dCINs responding to both medial and lateral MRF could also contribute to the non-predominant responses in MNs of the LMC or MMC. It is important to note that we have not yet determined how many of the dCINs that receive MRF inputs have synaptic connections onto MNs or how strong those connections are. Thus, although it is clear that the three dCIN populations provide a substrate for differential activation of MNs, their relative proportions cannot be equated with the strengths of the reticulospinal pathways involved.

Our results thus support the existence of single-crossed and double-crossed dCIN-mediated reticulospinal pathways to lumbar MNs originating from the MRF. In addition to dCINs, these pathways likely involve other groups of spinal INs because the ranges of response latencies in dCINs suggest the presence of monosynaptic and polysynaptic connections between medullary reticulospinal neurons and dCINs.

Methodological considerations

In this same preparation, Ca^{2+} transients elicited in spinal MNs by stimulation of vestibulospinal pathways occur one-to-one with action potentials (Kasumacic et al., 2010). Here, we used the presence of Ca^{2+} transients in MNs and dCINs as a general indicator of postsynaptic activity but could not gauge the relative contributions of suprathreshold and subthreshold events. Nor have we investigated the Ca^{2+} sources responsible for the transients, which could include voltage-sensitive calcium channels (Díaz-Ríos et al., 2007), calcium-permeable ligand-gated channels (Butt et al., 2002), and metabotropic glutamatergic and cholinergic receptors. We have previously discussed light scattering and spread of Ca^{2+} and/or Ca^{2+}-regulating second messengers through gap junctions as contributing factors to responses in MNs (Szokol et al., 2009). Here, light scattering from dCIN somata decreased by 80% within 25 μm, indicating that signal contamination among responsive dCINs is minor. This is in accord with the fact that many nonresponsive dCINs were located in close proximity to responsive dCINs. Regarding gap-junctions, there is evidence that dCINs are, to some extent, electrotonically coupled (Butt et al., 2002). Here, relatively common spontaneous Ca^{2+} transients (Figs. 7*D*, arrow; 9*B*) did not occur synchronously in all dCINs, suggesting that gap junctions between dCINs are spatially restricted. There is therefore reason to believe that the MRF-elicited Ca^{2+} signals in dCINs result primarily from synaptic activation, but the only way to resolve this is to monitor Ca^{2+} signals and synaptic potentials simultaneously with optical and intracellular recording.

Another technical issue, bearing on the assessment of response latencies, is that conduction velocities cannot be measured because the volley propagated in descending axons following MRF stimulation cannot be readily recorded in neonatal rodents (Szokol et al., 2008). Although the conduction velocity of medullary reticulospinal axons has not been determined in the neonatal mouse, it has been estimated that incompletely myelinated axons descending in the ventrolateral funiculus conduct at $\sim$0.5 ms^{-1} (Gordon and Whelan, 2008). With this speed and an average distance of 1.6 $\pm$ 0.03 cm between the MRF-stimulating electrode and the L2 segment, monosynaptic responses from reticulospinal axons with nontortuous trajectories would occur, at the earliest, at $\sim$35 ms (34 ms conduction time plus 1 ms synaptic delay at room temperature) (Lev-Tov and Pinco, 1992; Li and Burke, 2001), similar to the shortest response latencies we observed.

Are dCINs topographically organized according to their reticulospinal inputs?

We have previously estimated that the L2 segment of the E18.5 mouse embryo contains $\sim$800 dCINs, with axons projecting at

least to the L3/L4 border (Nissen et al., 2005). Here, we recorded dCINs with axons projecting at least as far as the L4 segment. If the estimate in E18.5 embryos holds for the neonate, then the 574 dCINs we recorded would provide very good coverage of the entire L2 dCIN population. Accordingly, we believe that the described response pattern is representative of the dCIN population as a whole.

This large sample size gave us a good opportunity to assess whether dCINs are topographically organized with respect to their reticulospinal inputs. Although we could not plot the locations of dCINs in the transverse plane using an absolute coordinate system due to variability among preparations in the angle of the obliquely cut face, we found that the majority of responsive dCINs was located ventral to the central canal. However, we found no obvious segregation of dCINs receiving different patterns of inputs from medial and lateral MRF. To approach a synthesis of topography and input–output relationships, it will be important in the future to relate the organization we have described here to patterns of other descending and sensory inputs, output patterns to trunk and hindlimb MNs, and neurotransmitter phenotypes.

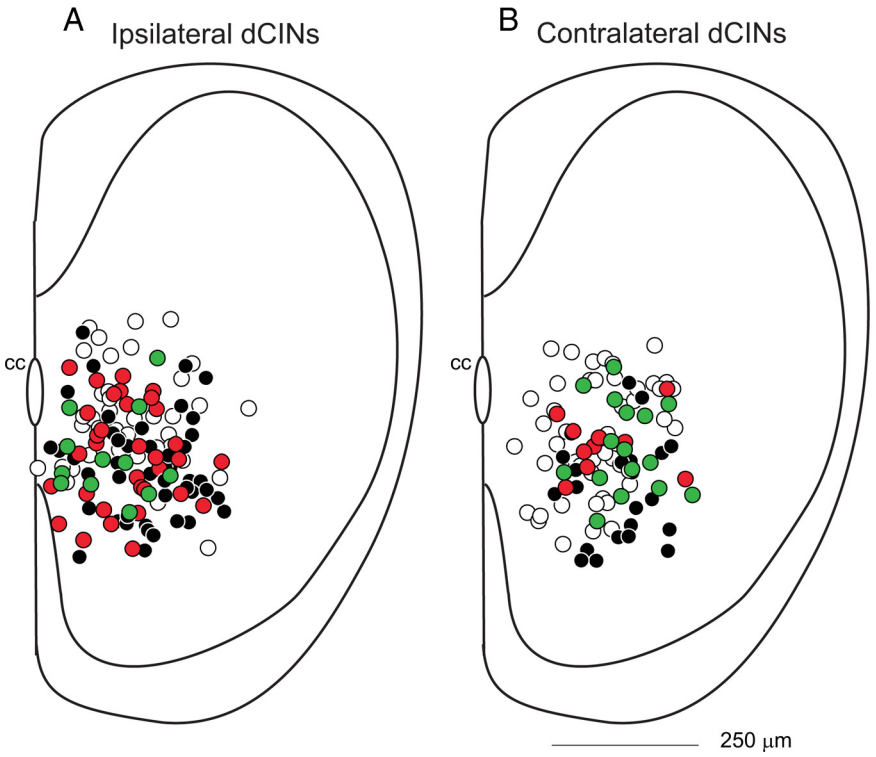

Figure 10. Spatial distribution of responsive and nonresponsive L2 dCINs. ***A***, ***B***, The position of individual ipsilateral (***A***) and contralateral (***B***) dCINs recorded was plotted on a representative section of the obliquely cut L2 segment. The dCINs were color-coded according to their responsiveness to MRF stimulation; the dCINs that responded to stimulation of the medial (28 of 224) and lateral (43 of 224) MRF only are shown as green and red circles, respectively, and the dCINs that responded to both medial and lateral MRF (67 of 224) and those that were nonresponsive (86 of 224) are shown as black and white circles, respectively. cc, Central canal. Scale bar: ***A*** and ***B***, 250 μm.

Comparison with previous studies in the adult cat

Our findings indicate that the medial and lateral MRF can activate ipsilateral and contralateral lumbar dCINs via both monosynaptic and polysynaptic connections, providing pathways that can exert crossed actions on trunk and hindlimb MNs. Regarding the ipsilateral dCINs, this suggests the presence of crossed dCIN-mediated pathways from medullary reticulospinal neurons to contralateral trunk and hindlimb MNs. Similar crossed CIN-mediated pathways from pontine reticulospinal neurons to hindlimb MNs have been described in the anesthetized adult cat (Jankowska et al., 2003, 2005, 2006). Regarding the contralateral dCINs, our findings are in accordance with the suggested presence in the adult cat of a dCIN-mediated double-crossed pathway between medullary reticulospinal neurons and ipsilateral hindlimb MNs (Jankowska et al., 2003; Matsuyama et al., 2004b). In addition, our findings suggest the presence of another dCIN-mediated double-crossed pathway between medullary reticulospinal neurons and ipsilateral trunk MNs. An important line of future inquiry will be the extent to which the crossed connections involve commissural reticulospinal axon collaterals (Matsuyama et al., 2004b) in addition to interposed dCINs. Tests of monosynapticity as well as anatomical studies will be required to evaluate this.

Several similarities exist in the connectivity between medullary reticulospinal neurons and the lumbar cord in the neonatal mouse and between medullary and pontine reticulospinal neurons and the lumbar cord in the adult cat. Further study is required to substantiate whether the organization of reticulospinal connectivity in the neonate mammal has already attained the general pattern seen in the adult, but our results here and in similar studies of the vestibulospinal system (Kasumacic et al., 2010) suggest that this may be the case. If so, the neonatal brainstem–spinal cord preparation would provide a very tractable experimental model for studying the organization of descending motor systems that could be directly extrapolated to the adult.

Potential functional roles of dCINs receiving MRF inputs

dCINs in the rostral lumbar spinal cord in rodents and cats are heterogeneous with respect to neurotransmitter phenotype and input–output connectivity (Jankowska, 2008; Restrepo et al., 2009 and references therein) and their functional roles during motor control remain incompletely described. For instance, whereas electrophysiological evidence suggests that dCINs play an important role in coordinating rostrocaudal, left–right synergies between hindlimb flexors and extensors such as during locomotion (Kiehn et al., 2008; Cowley et al., 2009), their role in coordinating synergies among axial muscles or between axial and hindlimb muscles during postural adjustments remains largely unexplored. The demonstration that dCINs receive functional reticulospinal inputs from both the medullary (present study) and the pontine (Jankowska et al., 2005) MRF is compatible with both roles. With respect to control of axial musculature and posture, a key finding here is that the lateral MRF, which activates predominantly trunk MNs, also activates dCINs. However, to assess the functional significance of this putative pathway, it will be important to determine whether dCINs make direct or indirect synaptic connections with MNs of the MMC.

Unraveling the complex interactions between the various groups of descending neurons and the large number of spinal neurons in mammals is a daunting task, but this study demonstrates that multineuron imaging facilitates the process dra-

matically. Further development of high throughput optical approaches will increase our capability to characterize the functional organization of extended brainstem-spinal cord motor networks in mammals.

References

Al-Mosawie A, Wilson JM, Brownstone RM (2007) Heterogeneity of V2-derived interneurons in the adult mouse spinal cord. Eur J Neurosci 26:3003–3015.

Alstermark B, Ogawa J (2004) In vivo recordings of bulbospinal excitation in adult mouse forelimb motoneurons. J Neurophysiol 92:1958–1962.

Alstermark B, Ogawa J, Isa T (2004) Lack of monosynaptic corticomotoneuronal EPSPs in rats: disynaptic EPSPs mediated via reticulospinal neurons and polysynaptic EPSPs via segmental interneurons. J Neurophysiol 91:1832–1839.

Brownstone RM, Wilson JM (2008) Strategies for delineating spinal locomotor rhythm-generating networks and the possible role of Hb9 interneurones in rhythmogenesis. Brain Res Rev 57:64–76.

Butt SJ, Kiehn O (2003) Functional identification of interneurons responsible for left-right coordination of hindlimbs in mammals. Neuron 38:953–963.

Butt SJ, Harris-Warrick RM, Kiehn O (2002) Firing properties of identified interneuron populations in the mammalian hindlimb central pattern generator. J Neurosci 22:9961–9971.

Cazalets JR, Borde M, Clarac F (1995) Localization and organization of the central pattern generator for hindlimb locomotion in newborn rat. J Neurosci 15:4943–4951.

Cowley KC, Zaporozhets E, Joundi RA, Schmidt BJ (2009) Contribution of commissural projections to bulbospinal activation of locomotion in the in vitro neonatal rat spinal cord. J Neurophysiol 101:1171–1178.

Deliagina TG, Orlovsky GN, Zelenin PV, Beloozerova IN (2006) Neural bases of postural control. Physiology 21:216–225.

Díaz-Ríos M, Dombeck DA, Webb WW, Harris-Warrick RM (2007) Serotonin modulates dendritic calcium influx in commissural interneurons in the mouse spinal locomotor network. J Neurophysiol 98:2157–2167.

Drew T, Prentice S, Schepens B (2004) Cortical and brainstem control of locomotion. Prog Brain Res 143:251–261.

Eide AL, Glover J, Kjaerulff O, Kiehn O (1999) Characterization of commissural interneurons in the lumbar region of the neonatal rat spinal cord. J Comp Neurol 403:332–345.

Floeter MK, Lev-Tov A (1993) Excitation of lumbar motoneurons by the medial longitudinal fasciculus in the in vitro brain stem spinal cord preparation of the neonatal rat. J Neurophysiol 70:2241–2250.

Floeter MK, Sholomenko GN, Gossard JP, Burke RE (1993) Disynaptic excitation from the medial longitudinal fasciculus to lumbosacral motoneurons: modulation by repetitive activation, descending pathways, and locomotion. Exp Brain Res 92:407–419.

Garcia-Rill E, Homma Y, Skinner RD (2004) Arousal mechanisms related to posture and locomotion. I. Descending modulation. Prog Brain Res 143:283–290.

Glover JC (1995) Retrograde and anterograde axonal tracing with fluorescent dextrans in the embryonic nervous system. Neurosci Protocols 30:1–13.

Gordon IT, Whelan PJ (2008) Brainstem modulation of locomotion in the neonatal mouse spinal cord. J Physiol 586:2487–2497.

Grillner S, Lund S (1968) The origin of a descending pathway with monosynaptic action on flexor motoneurones. Acta Physiol Scand 74:274–284.

Grillner S, Hongo T, Lund S (1968) Reciprocal effects between two descending bulbospinal systems with monosynaptic connections to spinal motoneurones. Brain Res 10:477–480.

Grillner S, Deliagina T, Ekeberg O, el Manira A, Hill RH, Lansner A, Orlovsky GN, Wallén P (1995) Neural networks that co-ordinate locomotion and body orientation in lamprey. Trends Neurosci 18:270–279.

Habaguchi T, Takakusaki K, Saitoh K, Sugimoto J, Sakamoto T (2002) Medullary reticulospinal tract mediating the generalized motor inhibition in cats. II. Functional organization within the medullary reticular formation with respect to postsynaptic inhibition of forelimb and hindlimb motoneurons. Neuroscience 113:65–77.

Hägglund M, Borgius L, Dougherty KJ, Kiehn O (2010) Activation of groups of excitatory neurons in the mammalian spinal cord or hindbrain evokes locomotion. Nat Neurosci 13:246–252.

Hinckley CA, Hartley R, Wu L, Todd A, Ziskind-Conhaim L (2005) Locomotor-like rhythms in a genetically distinct cluster of interneurons in the mammalian spinal cord. J Neurophysiol 93:1439–1449.

Jankowska E (1992) Interneuronal relay in spinal pathways from proprioceptors. Prog Neurobiol 38:335–378.

Jankowska E (2008) Spinal interneuronal networks in the cat: elementary components. Brain Res Rev 57:46–55.

Jankowska E, Edgley SA (2010) Functional subdivision of feline spinal interneurons in reflex pathways from group Ib and II muscle afferents: an update. Eur J Neurosci 32:881–893.

Jankowska E, Hammar I, Slawinska U, Maleszak K, Edgley SA (2003) Neuronal basis of crossed actions from the reticular formation on feline hindlimb motoneurons. J Neurosci 23:1867–1878.

Jankowska E, Edgley SA, Krutki P, Hammar I (2005) Functional differentiation and organization of feline midlumbar commissural interneurones. J Physiol 565:645–658.

Jankowska E, Stecina K, Cabaj A, Pettersson LG, Edgley SA (2006) Neuronal relays in double crossed pathways between feline motor cortex and ipsilateral hindlimb motoneurones. J Physiol 575:527–541.

Jankowska E, Bannatyne BA, Stecina K, Hammar I, Cabaj A, Maxwell DJ (2009) Commissural interneurons with input from group I and II muscle afferents in feline lumbar segments: neurotransmitters, projections and target cells. J Physiol 587:401–418.

Jordan LM, Liu J, Hedlund PB, Akay T, Pearson KG (2008) Descending command systems for the initiation of locomotion in mammals. Brain Res Rev 57:183–191.

Juvin L, Morin D (2005) Descending respiratory polysynaptic inputs to cervical and thoracic motoneurons diminish during early postnatal maturation in rat spinal cord. Eur J Neurosci 21:808–813.

Kasumacic N, Glover JC, Perreault MC (2010) Segmental patterns of vestibular-mediated synaptic inputs to axial and limb motoneurons in the neonatal mouse assessed by optical recording. J Physiol 588:4905–4925.

Kiehn O, Quinlan KA, Restrepo CE, Lundfald L, Borgius L, Talpalar AE, Endo T (2008) Excitatory components of the mammalian locomotor CPG. Brain Res Rev 57:56–63.

Kjaerulff O, Kiehn O (1996) Distribution of networks generating and coordinating locomotor activity in the neonatal rat spinal cord in vitro: a lesion study. J Neurosci 16:5777–5794.

Lanuza GM, Gosgnach S, Pierani A, Jessell TM, Goulding M (2004) Genetic identification of spinal interneurons that coordinate left-right locomotor activity necessary for walking movements. Neuron 42:375–386.

Lev-Tov A, Pinco M (1992) In vitro studies of prolonged synaptic depression in the neonatal rat spinal cord. J Physiol 447:149–169.

Li Y, Burke RE (2001) Short-term synaptic depression in the neonatal mouse spinal cord: effects of calcium and temperature. J Neurophysiol 85:2047–2062.

Lundfald L, Restrepo CE, Butt SJ, Peng CY, Droho S, Endo T, Zeilhofer HU, Sharma K, Kiehn O (2007) Phenotype of V2-derived interneurons and their relationship to the axon guidance molecule EphA4 in the developing mouse spinal cord. Eur J Neurosci 26:2989–3002.

Matsuyama K, Kobayashi Y, Takakusaki K, Mori S, Kimura H (1993) Termination mode and branching patterns of reticuloreticular and reticulospinal fibres of the nucleus reticularis pontis oralis in the cat: an anterograde PHA-L tracing study. Neurosci Res 17:9–21.

Matsuyama K, Takakusaki K, Nakajima K, Mori S (1997) Multi-segmental innervation of single pontine reticulospinal axons in the cervico-thoracic region of the cat: anterograde PHA-L tracing study. J Comp Neurol 377:234–250.

Matsuyama K, Mori F, Nakajima K, Drew T, Aoki M, Mori S (2004a) Locomotor role of the corticoreticular-reticulospinal-spinal interneuronal system. Prog Brain Res 143:239–249.

Matsuyama K, Nakajima K, Mori F, Aoki M, Mori S (2004b) Lumbar commissural interneurons with reticulospinal inputs in the cat: morphology and discharge patterns during fictive locomotion. J Comp Neurol 474:546–561.

Moran-Rivard L, Kagawa T, Saueressig H, Gross MK, Burrill J, Goulding M (2001) Evx1 is a postmitotic determinant of v0 interneuron identity in the spinal cord. Neuron 29:385–399.

Mori S, Iwakiri H, Homma Y, Yokoyama T, Matsuyama K (1995) Neuroanatomical and neurophysiological bases of postural control. Adv Neurol 67:289–303.

Nissen UV, Mochida H, Glover JC (2005) Development of projection-

specific interneurons and projection neurons in the embryonic mouse and rat spinal cord. J Comp Neurol 483:30–47.
Paxinos G, Halliday G, Watson C, Koutcherov Y, Wang H (2007) Atlas of the developing mouse brain. London: Elsevier.
Perreault MC, Kasumacic N, Glover JC, Szokol K (2009) Bulbospinal control of lumbar motor networks in the neonatal mouse. Paper presented at Groupe de recherche sur le système nerveux central, Montreal, May.
Peterson BW (1979) Reticulospinal projections to spinal motor nuclei. Annu Rev Physiol 41:127–140.
Peterson BW, Maunz RA, Pitts NG, Mackel RG (1975) Patterns of projection and braching of reticulospinal neurons. Exp Brain Res 23:333–351.
Peterson BW, Pitts NG, Fukushima K (1979) Reticulospinal connections with limb and axial motoneurons. Exp Brain Res 36:1–20.
Pierani A, Moran-Rivard L, Sunshine MJ, Littman DR, Goulding M, Jessell TM (2001) Control of interneuron fate in the developing spinal cord by the progenitor homeodomain protein Dbx1. Neuron 29:367–384.
Restrepo CE, Lundfald L, Szabó G, Erdélyi F, Zeilhofer HU, Glover JC, Kiehn O (2009) Transmitter-phenotypes of commissural interneurons in the lumbar spinal cord of newborn mice. J Comp Neurol 517:177–192.
Riddle CN, Edgley SA, Baker SN (2009) Direct and indirect connections with upper limb motoneurons from the primate reticulospinal tract. J Neurosci 29:4993–4999.
Sasaki S (1997) Axonal branching and termination of cervical reticulospinal neurons in the cat brachial segments. Neurosci Lett 228:83–86.
Sasaki S (1999) Direct connection of the nucleus reticularis gigantocellularis neurons with neck motoneurons in cats. Exp Brain Res 128:527–530.
Sasaki S, Yoshimura K, Naito K (2004) The neural control of orienting: role of multiple-branching reticulospinal neurons. Prog Brain Res 143:383–389.
Shapovalov AI (1969) Posttetanic potentiation of monosynaptic and disynaptic actions from supraspinal structures on lumbar motoneurons. J Neurophysiol 32:948–959.
Stokke MF, Nissen UV, Glover JC, Kiehn O (2002) Projection patterns of commissural interneurons in the lumbar spinal cord of the neonatal rat. J Comp Neurol 446:349–359.
Szokol K, Perreault MC (2009) Imaging synaptically mediated responses produced by brainstem inputs onto identified spinal neurons in the neonatal mouse. J Neurosci Methods 180:1–8.
Szokol K, Glover JC, Perreault MC (2008) Differential origin of reticulospinal drive to motoneurons innervating trunk and hindlimb muscles in the mouse revealed by optical recording. J Physiol 586:5259–5276.
Szokol K, Glover JC, Perreault MC (2009) Functional organization of reticulospinal inputs to lumbar commissural interneurons. Paper presented at SCRS, Madison, Wisconsin.
Vinay L, Cazalets JR, Clarac F (1995) Evidence for the existence of a functional polysynaptic pathway from trigeminal afferents to lumbar motoneurons in the neonatal rat. Eur J Neurosci 7:143–151.
Wilson JM, Hartley R, Maxwell DJ, Todd AJ, Lieberam I, Kaltschmidt JA, Yoshida Y, Jessell TM, Brownstone RM (2005) Conditional rhythmicity of ventral spinal interneurons defined by expression of the Hb9 homeodomain protein. J Neurosci 25:5710–5719.
Wilson VJ, Yoshida M (1969) Comparison of effects of stimulation of Deiters' nucleus and medial longitudinal fasciculus on neck, forelimb, and hindlimb motoneurons. J Neurophysiol 32:743–758.
Zhang Y, Narayan S, Geiman E, Lanuza GM, Velasquez T, Shanks B, Akay T, Dyck J, Pearson K, Gosgnach S, Fan CM, Goulding M (2008) V3 spinal neurons establish a robust and balanced locomotor rhythm during walking. Neuron 60:84–96.